

SOMO–HOMO Conversion in Triplet Carbenes

Ryo Murata, Zhe Wang, Yuki Miyazawa, Ivana Antol,* Shigeru Yamago, and Manabu Abe*

Cite This: *Org. Lett.* 2021, 23, 4955–4959

Read Online

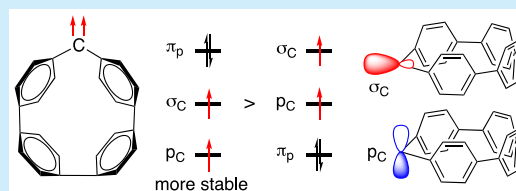
ACCESS |

Metrics & More

Article Recommendations

Supporting Information

ABSTRACT: In this study, the SOMO–HOMO conversion has been shown for the first time in triplet carbenes embedded in cycloparaphenylene units. The high-lying HOMO originating from the curved π -conjugated system and the low-lying SOMO–1 originating due to the small carbene angle are the key to endowing this interesting electronic configuration. Furthermore, simple planar triplet carbenes such as fluorenylidene were found to possess SOMO–HOMO energy-converted electronic configurations.



The Aufbau principle, Hund's rule, and Pauli exclusion principle determine the most stable electronic configuration in the ground state of molecules. According to these rules, the energy of the singly occupied molecular orbitals (SOMOs) of radicals should be higher than that of the doubly occupied molecular orbitals (DOMOs). Surprisingly, a few paramagnetic compounds such as metal complexes,¹ distonic radical anions,^{2–8} and stabilized radicals^{9–13} do not possess this normal electronic configuration. Rather, they exhibit a phenomenon called “SOMO–HOMO conversion”, in which the SOMO has a lower energy than the DOMO. This unusual electronic configuration plays an important role in switching the bond dissociation energy, generation of high-spin species in the oxidation state, and light emission in the near-infrared region. Although this phenomenon is very interesting, it is restricted to a limited group of compounds. In this work, we have conducted a computational study demonstrating the first example of SOMO–HOMO conversion in triplet carbenes **nC** ($n = 4–11$) and diarylcarbenes **F**, **CH₂**, **O**, and **NH** (Figure 1). Based on our observations, strategies were suggested for the molecular design of SOMO–HOMO energy-converted compounds.

Carbenes are well-known reactive intermediates¹⁴ not only in the field of fundamental chemistry^{15–17} but also in catalysis and high-spin materials.^{18–21} Diphenylcarbene (DPC) is a carbene prototype possessing a triplet ground state.^{22,23} As found in

experimental electron–nuclear-double-resonance (ENDOR) studies,²⁴ the twisted and bent structure of the triplet state was optimized at the UB3LYP/6-31G(d) level of theory (Figure 2a), with a carbene angle (θ_C) of 142.3°. The twist angle (θ_i) between the phenyl rings was 47.2°. The energetic preference of the triplet state over the closed-shell and open-shell singlets was computed to be 7.4 and 4.5 kcal mol^{−1}, respectively, at the same level of theory. The open-shell singlet state was computed using the broken-symmetry (BS)²⁵ approach for the DFT calculations. As expected, the two singly occupied orbitals in the triplet state, SOMO ($p_{C,DPC}$, −4.60 eV) and SOMO–1 ($\sigma_{C,DPC}$, −5.74 eV), were higher in energy than the HOMO (−6.99 eV for α -spin and −6.76 eV for β -spin). The matching of α -spin and β -spin orbitals was determined by comparing the energy of α -spin and β -spin orbitals and subjectively choosing orbitals that looked similar to each other. Intriguingly, triplet carbenes (**nC**) embedded in the curved cycloparaphenylenes (CPPs) such as **4C** ($n = 4$) do not follow the Aufbau principle (Figure 2b,c). The carbene angles of **4C** in the fully optimized C_1 and C_{2v} symmetries, i.e., **4C_{C1}** and **4C_{C2v}**, were computed to be 127.9° and 125.9°, respectively, which were $\sim 20^\circ$ smaller than that of DPC. The C_1 structure was lower in energy by 0.58 kcal mol^{−1} than the C_{2v} structure. The twist angles between the two benzene rings at the carbene center were 6.8° and 0.0° in **4C_{C1}** and **4C_{C2v}**, respectively, indicating that the two benzene rings are oriented parallelly. The energetic preference of the triplet state over the closed-shell/open-shell singlets was computed to be 3.3/1.3 in the C_1 symmetry. The singly occupied orbital SOMO–1 (p_{C4C} , −5.79 eV) was located at a lower energy than HOMO (−4.81 eV for α -spin and −4.86 eV for β -spin) in fully optimized **4C_{C1}** (Figure 2b), while in **4C_{C2v}** (Figure 2c), both SOMO (σ_{C4C} ,

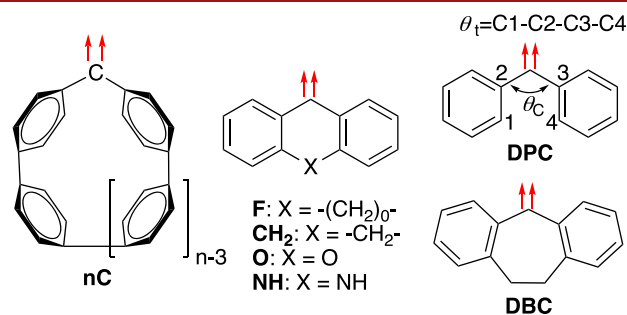
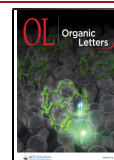


Figure 1. Structures of **nC**, **F**, **CH₂**, **O**, **NH**, **DPC**, and **DBC**.

Received: April 2, 2021
 Published: May 28, 2021



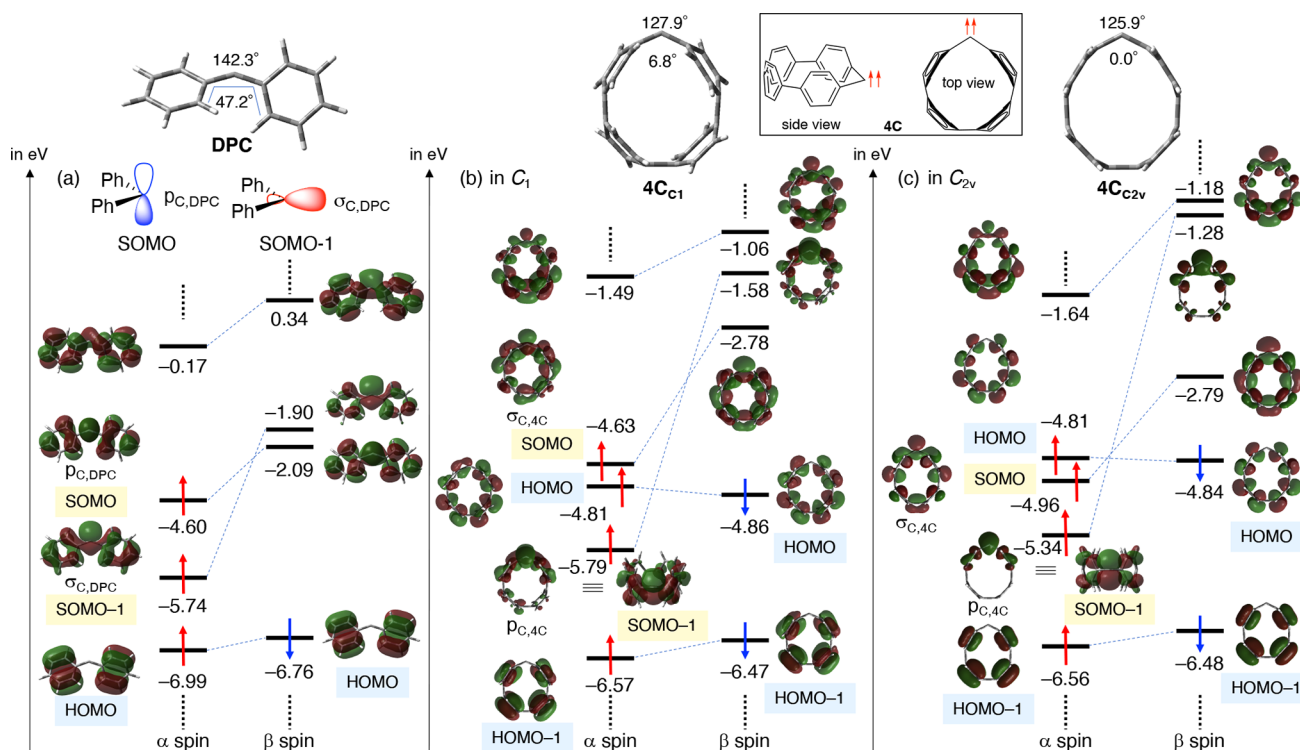


Figure 2. Molecular orbital diagrams of DPC (a), $4C_{C_1}$ in C_1 symmetry (b), and $4C_{C_{2v}}$ in C_{2v} symmetry (c) at the UB3LYP/6-31G(d) level.

−4.96 eV) and SOMO−1 ($p_{C_{4C}}$ −5.34 eV) were at a lower energy than HOMO (−4.81 eV for α -spin and −4.84 eV for β -spin). The similar SOMO–HOMO level conversion was calculated at the UCAM-B3LYP/6-31G(d) and U ω B97XD/6-31G(d) level of theories (Figure S5).

It should be noted that the carbene orbital, p_C , is SOMO in DPC but SOMO−1 in $4C$. Thus, SOMO−1 in DPC is another carbene orbital, σ_C . Evidently, σ_C is SOMO in $4C$. To understand this intriguing phenomenon, the linear p -quaterphenyl-substituted carbene $4Ph_{125}$ in C_2 symmetry with parallelly oriented benzene rings was computed by fixing the carbene angle at 125° and the parallel orientation of the benzene rings at the same level of theory (Figure 3a). The SOMO (σ_C) and SOMO−1 (p_C) energies (−5.20 and −5.41 eV,

respectively) were higher than that of HOMO (−5.63 eV; Figure S1). This indicated that $4Ph_{125}$ followed the Aufbau principle despite the decreased SOMO–HOMO energy spacing relative to that in DPC (Figure 2a). The SOMO(σ_C)–SOMO−1(p_C) energy order was the same as that of $4C$, not DPC. The HOMO energy increased by about 1.3 eV compared to the HOMO energy of DPC, and this increase is not enough for the SOMO–HOMO conversion. Therefore, the intriguing phenomenon in $4C$ occurs due to the significant increase in the HOMO energy due to the curved π -electron systems and the increased π -conjugation (Figure 3b). Thus, the HOMO energy in $4C$ was higher than that in DPC by ~ 2 eV. A similar effect, i.e., increased HOMO energy due to curved π -electron systems, has been observed for cycloparaphenylene (CPP) derivatives.²⁶

The switch in the order of SOMO and SOMO−1 energy can be explained on the basis of orbital interactions of σ_C and p_C with π_p and σ_p in $4C$ (Figure 3c). The low-lying σ_C orbital due to the small carbene angle can interact with the high-lying π_p orbital (the interaction is indicated in red) and switch the position of $\sigma_{C_{4C}}$ (SOMO) and $p_{C_{4C}}$ (SOMO−1), whose energy level is determined by the interaction of the p_C orbital with the σ_p orbital (the interactions are indicated in blue).

Next, the effect of size was examined for the SOMO–HOMO conversion in triplet carbenes nC (Figure 4). In C_{2v} symmetry featuring the parallel orientation of the benzene rings, carbenes 4 – $11C_{C_{2v}}$ possessed the SOMO–HOMO converted electronic configuration, although the SOMO and HOMO energies were largely dependent on the size of the cycloparaphenylene unit (Figure 4a). Thus, the SOMO (σ_C , red color) was energetically stabilized from −4.62 eV ($11C_{C_{2v}}$) to −4.96 eV ($4C_{C_{2v}}$) upon decreasing the number of benzene rings, while the HOMO was energetically destabilized (π in CPP ring, black color) from −5.04 eV ($11C_{C_{2v}}$) to −4.82 eV ($4C_{C_{2v}}$) upon decreasing the ring size. The decrease in SOMO energy can be reasonably explained by the decrease in carbene angle θ_C , which affects the s

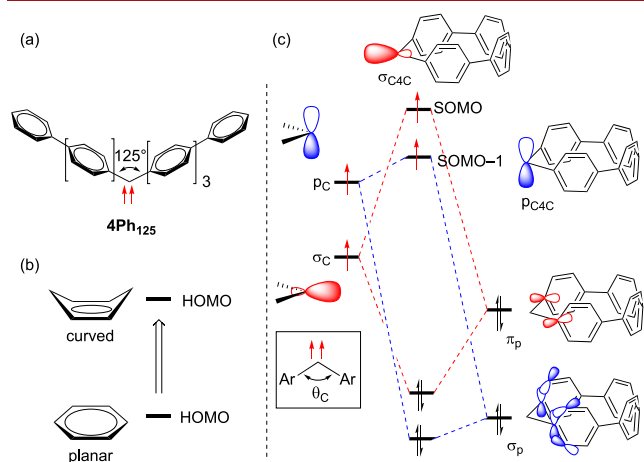


Figure 3. (a) Molecular structure of $4Ph_{125}$. (b) Increase in HOMO energy due to the curved system. (c) Orbital interactions of p_C and σ_C with π_C and σ_p .

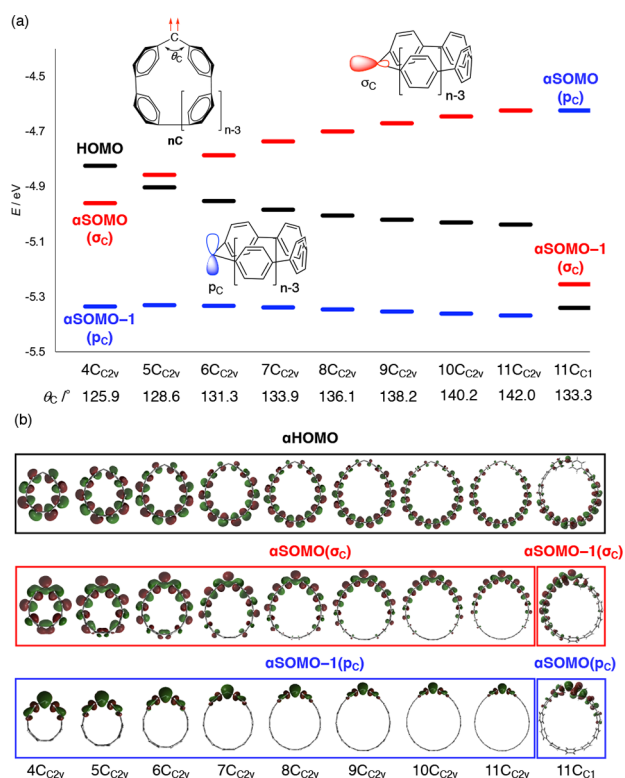


Figure 4. (a) Effect of size on the energy level of α -SOMO, α -SOMO-1, HOMO, and carbene angle (θ_c) in nC_{2v} . The average value of α -spin and β -spin orbital energy is used as the HOMO energy. (b) α -SOMO, α -SOMO-1, and α -HOMO orbitals in nC_{2v} .

character of σ_C . According to the natural bond orbital (NBO) analysis,²⁷ the s character increased from 18.6% ($11C_{2v}$) to

26.3% ($4C_{2v}$) (Table S1). As evident from the curve effect of π -conjugated systems,^{26,28} the quinoidal contribution increased with decreasing ring size. Thus, the HOMO energy increased despite the decrease in the number of benzene rings. In contrast, the energy of SOMO-1 (p_C , blue color) was not largely affected by the ring size (Figure 4a). This is reasonable because the energy and orientation of adjacent benzene σ -orbitals in C_{2v} (σ_p , Figure 3c) should not be affected by the ring size.

Interestingly, the fully optimized C_1 structure of $11C_{C1}$ showed the normal electronic configuration— $\cdots(HOMO)^2(SOMO-1)^1(SOMO)^1\cdots$ (right end in Figure 4a). The SOMO-SOMO-1 energy order switched from σ_C - p_C to the normal p_C - σ_C found in DPC because the orbital interaction of σ_C and π_p becomes weak due to the twisted conformation of the two phenyl rings adjacent to the carbene center in C_1 symmetry. The computed twist angle and carbene angle were 55.1° and 133.3° in $11C_{C1}$, respectively. The energetic preference of the triplet state over the closed-shell and open-shell singlets was computed to be 4.9 and 1.6 kcal mol⁻¹, respectively. In fully optimized C_1 symmetry, triplet carbenes 4–8 C_{C1} were also found to possess the SOMO-HOMO-converted electronic configuration (Figure S2a). However, it is difficult to determine whether triplet carbenes 9,10 C_{C1} possess the SOMO-HOMO converted electronic configuration (Figure S2b). The SOMO and HOMO energies are largely dependent upon the carbene angle and twisted angles of the two benzene rings.

Why does an electron in HOMO not fall down to the low-lying SOMO-1 to generate the normal electronic configuration? As seen in Figure 4b, SOMO-1 (σ_C) is localized at the carbene center, while the HOMO is highly delocalized in the π -conjugated system. Thus, the two electrons preferably occupy the more delocalized HOMO than the relatively localized SOMO-1 to avoid electronic repulsion.

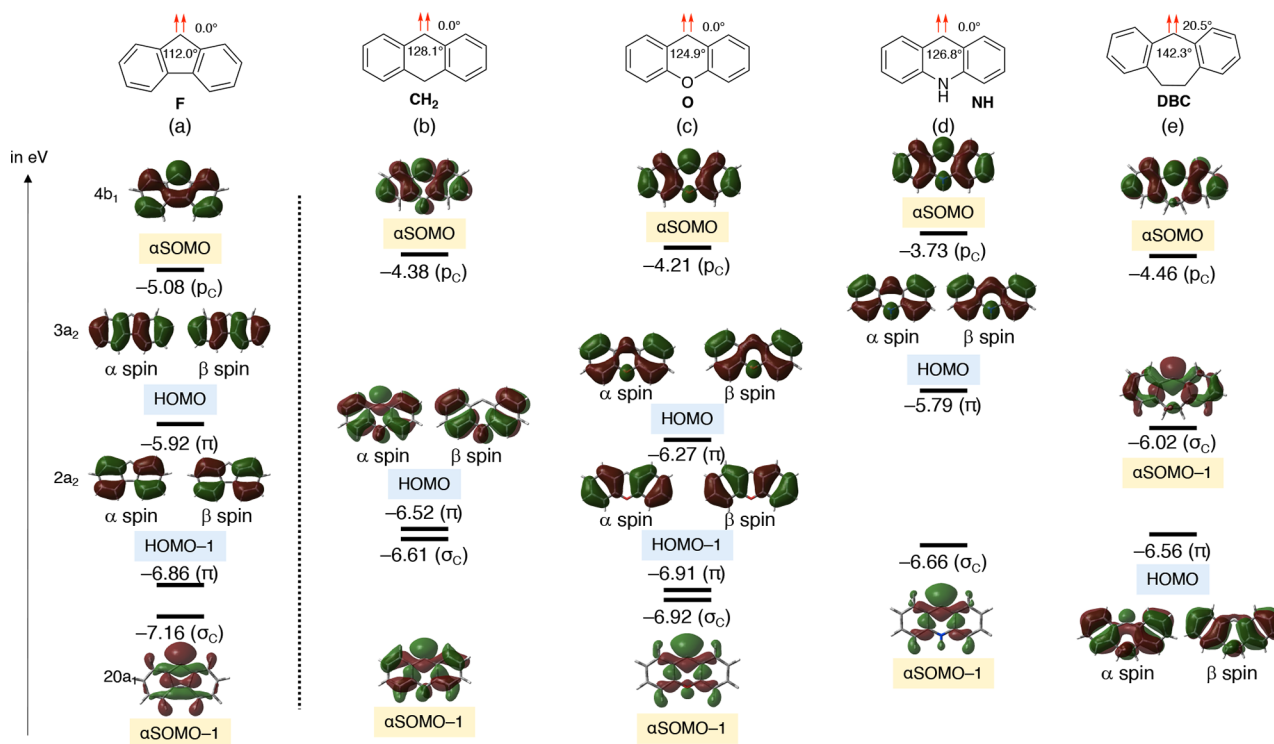


Figure 5. Molecular orbital diagrams for α -spin of F (a), CH_2 (b), O (c), NH (d), and DBC (e) at the UB3LYP/6-31G(d) level of theory. The average value of α -spin and β -spin orbital energy is used as the HOMO energy.

Surprisingly, a simple carbene, fluorenylidene (F),^{29,30} in C_{2v} symmetry with a small carbene angle of 112.0° also exhibited the SOMO–HOMO energy conversion phenomenon at the UB3LYP/6-31G(d) level of theory (Figure 5a). The energetic preference of the triplet state over the closed-shell and open-shell singlets was computed to be 6.6 and 3.4 kcal mol⁻¹, respectively. The triplet ground state was experimentally reported by Wasserman, Schuster, Platz, and Scaiano.^{31,32} The low-lying α -SOMO–1 (σ_C , $20a_1$, -7.16 eV) was lower in energy than both HOMO–1 ($2a_2$, -6.86 eV) and HOMO ($3a_2$, -5.92 eV). α SOMO (P_C , $4b_1$) energy was computed to be -5.08 eV. The complete active space second-order perturbation theory³³ at the CASPT2/CASSCF(14,14)/cc-pVDZ wavefunction demonstrated that the 1^3B_1 state, $\dots(20a_1)^1(2a_2)^2(3a_2)^2(4b_1)^1\dots$ (Figure 5a), is more stable by 1.94 and 2.91 eV than the triplet 1^3B_2 state, $\dots(20a_1)^2(2a_2)^2(3a_2)^1(4b_1)^1\dots$, and the 2^3B_2 state, $\dots(20a_1)^2(2a_2)^1(3a_2)^2(4b_1)^1\dots$, respectively.

To understand the generality of the SOMO–HOMO conversion phenomenon in triplet carbenes, several diarylcarbenes, CH_2 ($X = CH_2$),³⁴ O ($X = O$),³⁴ and NH ($X = NH$)³⁴ in C_s symmetry and DBC³⁵ in C_2 symmetry, in addition to planar carbene F, were computed at the UB3LYP/6-31G(d) level of theory (Figures 5b–e). Surprisingly, the SOMO–HOMO conversion was observed in planar triplet carbenes CH_2 , O , and NH featuring the relatively small carbene angles (θ_C), although the HOMO and SOMO–1 are degenerated in CH_2 (Figure 5b). The SOMO (σ_C) energy decreases with decreasing carbene angle θ_C because the s character increases. The HOMO energy of -5.79 eV in NH was higher than that (-6.52 eV) in CH_2 due to the electron-donating lone pair at the nitrogen atom (Figure 5d).

The HOMO energy (-6.27 eV) in O was lower than NH (Figure 5c). Twisted carbene DBC ($\theta_C = 142.3^\circ$) with the twisted angle of 20.5° was found to possess the normal electronic configuration, similar to DPC. Thus, the carbene angle θ_C and the heteroatom effect on the HOMO energy are the key to generate the SOMO–HOMO conversion (Figure 6).

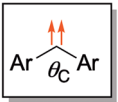
	SOMO–HOMO θ_C (°) conversion	
DPC	142.3	NO
F: X = $-(CH_2)_0-$	112.0	} YES
CH_2 : X = $-CH_2-$	128.1	
O: X = O	124.9	
NH: X = NH	126.8	
DBC	142.3	NO

Figure 6. SOMO–HOMO conversion in triplet diarylcarbenes.

The energetic preference of the triplet state of CH_2 over the closed-shell/open-shell singlets was computed to be 2.6/1.1 kcal mol⁻¹.³⁴ In the case of DBC, the energetic preference of the triplet state over the closed-shell singlet was computed to be 11.4 kcal mol⁻¹. The singlet ground state was computed for O and NH with the singlet preference of 6.8 and 8.6 kcal mol⁻¹, respectively, at the same of level of theory.³⁴

In summary, the SOMO–HOMO energy conversion phenomenon was examined for the first time in triplet diarylcarbenes. Triplet carbenes 4– $8C_{C1}$ and 4– $11C_{C2v}$ with

the curved π -conjugated cycloparaphenylene structure and planar carbenes F, CH_2 , O , and NH possessed the SOMO–HOMO converted electronic configuration as their most stable electronic configuration. Diarylcarbenes such as $11C_{C1}$, DPC, and DBC with the twisted conformation and relatively large carbene angles did not exhibit the SOMO–HOMO conversion phenomenon. This computational study revealed one of the guidelines for molecular design of SOMO–HOMO converted compounds. One of the possible experiments to prove the computational prediction would be two-electron oxidation. The SOMO–HOMO level converted triplet-carbenes would give triplet species after the oxidation, although the singlet species is expected to be generated in the oxidation of normal triplet carbenes. To understand the chemistry deeply, further experimental and computational studies are needed in the future.

■ ASSOCIATED CONTENT

Supporting Information

The Supporting Information is available free of charge at <https://pubs.acs.org/doi/10.1021/acs.orglett.1c01137>.

Computational details (PDF)

■ AUTHOR INFORMATION

Corresponding Authors

Manabu Abe – Department of Chemistry, Graduate School of Science, Hiroshima University, Higashi-Hiroshima 739-8526, Hiroshima, Japan; orcid.org/0000-0002-2013-4394; Email: mabe@hiroshima-u.ac.jp

Ivana Antol – Laboratory for Physical Organic Chemistry, Division of Organic Chemistry and Biochemistry, Ruđer Bošković Institute, 10000 Zagreb, Croatia; Email: ivana.antol@irb.hr

Authors

Ryo Murata – Department of Chemistry, Graduate School of Science, Hiroshima University, Higashi-Hiroshima 739-8526, Hiroshima, Japan

Zhe Wang – Department of Chemistry, Graduate School of Science, Hiroshima University, Higashi-Hiroshima 739-8526, Hiroshima, Japan; orcid.org/0000-0002-9996-586X

Yuki Miyazawa – Department of Chemistry, Graduate School of Science, Hiroshima University, Higashi-Hiroshima 739-8526, Hiroshima, Japan

Shigeru Yamago – Institute for Chemical Research, Kyoto University, Kyoto 611-0011, Japan; orcid.org/0000-0002-4112-7249

Complete contact information is available at: <https://pubs.acs.org/doi/10.1021/acs.orglett.1c01137>

Notes

The authors declare no competing financial interest.

■ ACKNOWLEDGMENTS

This work was supported by JSPS KAKENHI Grant Numbers 17H03022 (MA), 20K21197 (MA), and 16H06352 (SY) and also supported by the International Collaborative Research Program of Institute for Chemical Research, Kyoto University (grant 2020-43).

REFERENCES

- (1) Westcott, B. L.; Gruhn, N. E.; Michelsen, L. J.; Lichtenberger, D. L. Experimental Observation of Non-Aufbau Behavior: Photoelectron Spectra of Vanadyl octaethylporphyrinate and Vanadylphthalocyanine. *J. Am. Chem. Soc.* **2000**, *122* (33), 8083–8084.
- (2) Gryn'ova, G.; Coote, M. L. Origin and Scope of Long-Range Stabilizing Interactions and Associated SOMO–HOMO Conversion in Distonic Radical Anions. *J. Am. Chem. Soc.* **2013**, *135* (41), 15392–15403.
- (3) Gryn'ova, G.; Marshall, D. L.; Blanksby, S. J.; Coote, M. L. Switching Radical Stability by p H-Induced Orbital Conversion. *Nat. Chem.* **2013**, *5* (6), 474–481.
- (4) Franchi, P.; Mezzina, E.; Lucarini, M. SOMO-HOMO Conversion in Distonic Radical Anions: An Experimental Test in Solution by EPR Radical Equilibration Technique. *J. Am. Chem. Soc.* **2014**, *136* (4), 1250–1252.
- (5) Kumar, A.; Sevilla, M. D. Proton Transfer Induced SOMO-to-HOMO Level Switching in One-Electron Oxidized A-T and G-C Base Pairs: A Density Functional Theory Study. *J. Phys. Chem. B* **2014**, *118* (20), 5453–5458.
- (6) Kumar, A.; Sevilla, M. D. SOMO–HOMO Level Inversion in Biologically Important Radicals. *J. Phys. Chem. B* **2018**, *122* (1), 98–105.
- (7) So, S.; Kirk, B. B.; Wille, U.; Trevitt, A. J.; Blanksby, S. J.; da Silva, G. Reactions of a Distonic Peroxyl Radical Anion Influenced by SOMO–HOMO Conversion: An Example of Anion-Directed Channel Switching. *Phys. Chem. Chem. Phys.* **2020**, *22* (4), 2130–2141.
- (8) Kasemthaveechok, S.; Abella, L.; Jean, M.; Cordier, M.; Roisnel, T.; Vanthuynne, N.; Guizouarn, T.; Cador, O.; Autschbach, J.; Crassous, J.; Favereau, L. Axially and Helically Chiral Cationic Radical Bicarbazoles: SOMO-HOMO Level Inversion and Chirality Impact on the Stability of Mono- And Diradical Cations. *J. Am. Chem. Soc.* **2020**, *142* (48), 20409–20418.
- (9) Kusamoto, T.; Kume, S.; Nishihara, H. Realization of SOMO–HOMO Level Conversion for a TEMPO-Dithiolate Ligand by Coordination to Platinum(II). *J. Am. Chem. Soc.* **2008**, *130* (42), 13844–13845.
- (10) Kusamoto, T.; Kume, S.; Nishihara, H. Cyclization of TEMPO Radicals Bound to Metalladithiolene Induced by SOMO-HOMO Energy-Level Conversion. *Angew. Chem., Int. Ed.* **2010**, *49* (3), 529–531.
- (11) Sugawara, T.; Komatsu, H.; Suzuki, K. Interplay between Magnetism and Conductivity Derived from Spin-Polarized Donor Radicals. *Chem. Soc. Rev.* **2011**, *40* (6), 3105.
- (12) Tanushi, A.; Kimura, S.; Kusamoto, T.; Tominaga, M.; Kitagawa, Y.; Nakano, M.; Nishihara, H. NIR Emission and Acid Induced Intramolecular Electron Transfer Derived from a SOMO-HOMO Converted Non-Aufbau Electronic Structure. *J. Phys. Chem. C* **2019**, *123*, 4417–4423.
- (13) Guo, H.; Peng, Q.; Chen, X.-K.; Gu, Q.; Dong, S.; Evans, E. W.; Gillett, A. J.; Ai, X.; Zhang, M.; Credgington, D.; Coropceanu, V.; Friend, R. H.; Brédas, J.-L.; Li, F. High stability and luminescence efficiency in donor–acceptor neutral radicals not following the Aufbau principle. *Nat. Mater.* **2019**, *18* (9), 977–984.
- (14) *Contemporary Carbene Chemistry*; Moss, R. A., Doyle, M. P., Eds.; John Wiley & Sons: Hoboken, 2014.
- (15) Yakiyama, Y.; Wang, Y.; Hatano, S.; Abe, M.; Sakurai, H. Generation of “Sumanenylidene”: A Ground-State Triplet Carbene on a Curved π -Conjugated Periphery. *Chem. - Asian J.* **2019**, *14* (10), 1844–1848.
- (16) Trosien, I.; Mendez-Vega, E.; Thomanek, T.; Sander, W. Conformational Spin Switching and Spin-Selective Hydrogenation of a Magnetically Bistable Carbene. *Angew. Chem.* **2019**, *131* (42), 14997–15001.
- (17) Zhu, Z.; Bally, T.; Stracener, L. L.; McMahon, R. J. Reversible Interconversion between Singlet and Triplet 2-Naphthyl-(Carbomethoxy)Carbene. *J. Am. Chem. Soc.* **1999**, *121* (12), 2863–2874.
- (18) Vivancos, Á.; Segarra, C.; Albrecht, M. Mesoionic and Related Less Heteroatom-Stabilized N-Heterocyclic Carbene Complexes: Synthesis, Catalysis, and Other Applications. *Chem. Rev.* **2018**, *118* (19), 9493–9586.
- (19) Peris, E. Smart N-Heterocyclic Carbene Ligands in Catalysis. *Chem. Rev.* **2018**, *118* (19), 9988–10031.
- (20) Hirai, K.; Itoh, T.; Tomioka, H. Persistent Triplet Carbenes. *Chem. Rev.* **2009**, *109* (8), 3275–3332.
- (21) Bourissou, D.; Guerret, O.; Gabbai, F. P.; Bertrand, G. Stable Carbenes. *Chem. Rev.* **2000**, *100* (1), 39–91.
- (22) Murray, R. W.; Trozzolo, A. M.; Wasserman, E.; Yager, W. A.; Murray, R. W.; Trozzolo, A. M.; Wasserman, E.; Yager, W. A. *J. Am. Chem. Soc.* **1962**, *84* (16), 3213–3214.
- (23) Hutchison, C. A.; Kohler, B. E. Electron Nuclear Double Resonance in an Organic Molecule in a Triplet State. Spin Densities in Fluorenylidene in Diazofluorene Single Crystals. *J. Chem. Phys.* **1969**, *51* (8), 3327–3335.
- (24) Doetschman, D. C.; Hutchison, C. A. Electron Paramagnetic Resonance and Electron Nuclear Double Resonance Studies of the Chemical Reactions of Diphenyldiazomethane and of Diphenylmethylene in Single 1,1-Diphenylethylene Crystals. *J. Chem. Phys.* **1972**, *56* (8), 3964–3982.
- (25) Yamaguchi, K.; Jensen, F.; Dorigo, A.; Houk, K. N. A Spin Correction Procedure for Unrestricted Hartree-Fock and Møller-Plesset Wavefunctions for Singlet Diradicals and Polyradicals. *Chem. Phys. Lett.* **1988**, *149* (5–6), 537–542.
- (26) (a) Iwamoto, T.; Watanabe, Y.; Sakamoto, Y.; Suzuki, T.; Yamago, S. Selective and Random Syntheses of [n]-Cycloparaphenylenes (n = 8–13) and Size Dependence of Their Electronic Properties. *J. Am. Chem. Soc.* **2011**, *133* (21), 8354–8361. (b) Miyazawa, Y.; Wang, Z.; Matsumoto, M.; Hatano, S.; Antol, I.; Kayahara, E.; Yamago, S.; Abe, M. 1,3-Diradicals Embedded in Curved Paraphenylene Units: Singlet versus Triplet State and In-Plane Aromaticity. *J. Am. Chem. Soc.* **2021**, *143* (19), 7426–7439.
- (27) Carpenter, J. E.; Weinhold, F. Analysis of the Geometry of the Hydroxymethyl Radical by the “Different Hybrids for Different Spins” Natural Bond Orbital Procedure. *J. Mol. Struct.: THEOCHEM* **1988**, *169* (C), 41–62.
- (28) Darzi, E. R.; Jasti, R. The Dynamic, Size-Dependent Properties of [5]-[12]Cycloparaphenylenes. *Chem. Soc. Rev.* **2015**, *44* (18), 6401–6410.
- (29) Trozzolo, A. M.; Murray, R. W.; Wasserman, E. The Experimental Conditions (Ir/Ph₃P) THE ELECTRON PARAMAGNETIC RESONANCE OF REACTION ASSOCIATED WITH A GROUND STATE Sir: Hydroboration Recently Has Gained Prominence. *J. Am. Chem. Soc.* **1962**, *84* (1), 4990–4911.
- (30) Senthilnathan, V. P.; Platz, M. S. Determination of the Absolute Rates of Decay of Arylcarbenes in Various Low Temperature Matrices by Electron Spin Resonance Spectroscopy. *J. Am. Chem. Soc.* **1980**, *102* (26), 7637–7643.
- (31) Grasse, P. B.; Brauer, B. E.; Zupancic, J. J.; Kaufmann, K. J.; Schuster, G. B. Chemical and Physical Properties of Fluorenylidene: Equilibration of the Singlet and Triplet Carbenes. *J. Am. Chem. Soc.* **1983**, *105* (23), 6833–6845.
- (32) Griller, D.; Hadel, L.; Nazran, A. S.; Platz, M. S.; Wong, P. C.; Savino, T. G.; Scaiano, J. C. Fluorenylidene: Kinetics and Mechanism. *J. Am. Chem. Soc.* **1984**, *106* (8), 2227–2235.
- (33) Andersson, K. Different Forms of the Zeroth-Order Hamiltonian in Second-Order Perturbation Theory with a Complete Active Space Self-Consistent Field Reference Function. *Theor. Chim. Acta* **1995**, *91* (1–2), 31–46.
- (34) Li, Y. Z.; Schuster, G. B. Semiempirical Calculations of Carbenes with Aromatic Substituents: A Comparison of Theory with Experiment. *J. Org. Chem.* **1988**, *53* (6), 1273–1277.
- (35) Moritani, I.; Murahashi, S.; Nishino, M.; Yamamoto, Y.; Itoh, K.; Mataga, N. The Electron Spin Resonance of Triplet Dihydrodibenzo-[u,i]Cycloheptenylidene, Dibenzo[a,i]Cycloheptenylidene, and Tribenzo[a,c,e]Cycloheptenylidene. *J. Am. Chem. Soc.* **1967**, *89* (5), 1259–1260.